Quinine: re-designed and re-routed

Chinazom Precious Agbo (chinazom.agbo@unn.edu.ng)
University of Nigeria
Timothy Chukwuebuka Ugwuanyi
University of Nigeria
Osita Christopher Eze
University of Nigeria
Adaeze Linda Onugwu
University of Nigeria
Adaeze Chidiebere Echezona
University of Nigeria
Chinekwu Sherridan Nwagwu
University of Nigeria
Samuel Wisdom Uzondu
University of Nigeria
John Dike Ogbonna
University of Nigeria
Lydia Onyinyechi Ugorji
University of Nigeria
Petra Obioma Nnamani
University of Nigeria
Paul Achile Akpa
University of Nigeria
Joy Nneji Reginald-Opara
University of Nigeria
Christopher McConville
University of Birmingham, United Kingdom
Anthony Amaechi Attama
University of Nigeria
Kenneth Chibuzor Ofokansi
University of Nigeria

Research Article

Keywords: severe malaria, cerebral malaria, quinine hydrochloride, intranasal route, nanostructured lipid carriers, solidified reverse micellar solutions, Phospholipon® 90H, Softisan® 154, Compritol®.

Posted Date: September 6th, 2022

DOI: https://doi.org/10.21203/rs.3.rs-2018587/v1

Abstract

Quinine (QHCl) as an antimalarial drug has remained very relevant 400 years after its effectiveness was discovered. Unlike other antimalarials, the development of resistance to quinine has been slow. Hence, this drug is till date still used for the treatment of severe and cerebral malaria, for malaria treatment in all trimesters of pregnancy, and in combination with doxycycline against multi-drug resistant parasites. The declined in its administration over the years is mainly associated with poor tolerability due to its gastrointestinal (GIT) side effects such as cinchonism, complex dosing regimen and bitter taste, all of which result in poor compliance. Hence our research was aimed at redesigning quinine using nanotechnology and investigating an alternative route for its administration for the treatment of malaria. A nanosuspension (NS) of QHCl was formulated to suit intranasal administration. QHCl-NS was prepared using lipid matrices made up of solidified reverse micellar solutions (SRMS) comprising Phospholipon® 90H and lipids (Softisan® 154 or Compritol®) in 1:2 ratio, while Poloxamer® 188 (P188) and Tween® 80 (T80) were used as stabilizer and surfactant. The QHCl-NS formulated were in nanosize range (68.6±0.86 to 300.8±10.11 nm), and highly stable during storage. QHCl-NS achieved above 80 % in vitro drug release in 6 h. Ex vivo permeation studies revealed that formulating QHCl as NS resulted in a 5-fold and 56- fold increase in flux and permeation coefficient, respectively, thereby enhancing permeation through pig nasal mucosa better than plain drug solutions. This implies that the rate of absorption as well as ease of drug permeation through porcine nasal mucosa was impressively enhanced by formulating QHCl as NS. Most importantly, reduction in parasitaemia in mice infected with plasmodium berghei ANKA by QHCl-NS administered through the intranasal route (51.16 %) was comparable to oral administration (52.12 %). Therefore, redesigning QHCl as NS for intranasal administration has great potentials to serve as a more tolerable options for the treatment of malaria in endemic areas.

1. Introduction

The discovery of quinine in 17th century and its use for malaria treatment was the first successful use of a chemical compound to treat an infectious disease. Unlike other antimalarials, the development of resistance to quinine (QHCl) has been slow, with the first report released in 1910 [1], hence its use has continued till date. The declined in its administration over the years is mainly associated with poor tolerability due to its gastrointestinal side effects such as cinchonism (nausea, vomiting, dysphoria, tinnitus, and high-tone deafness. Adverse events such as hypoglycemia is also associated with quinine use especially in pregnancy. Other drawbacks of quinine include its complex dosing regimen and bitter taste, all of which result in poor compliance [1]. Despite these shortcomings of quinine, its use has continued till date because of its defiance to resistance by malaria parasite. Intravenous (IV) quinine still finds use as second line treatment for severe malaria, after IV artesunate [2]. Quinine is considered safe for malaria treatment in all trimesters of pregnancy. Quinine in combination with doxycycline is effective against multi-drug resistant parasites. Doxycycline is also associated with gastrointestinal side effects and may reduce the compliance of patients to both drugs [3]. Another important advantage of quinine compared to other antimalarials is its affordability, this is a major deciding factor in most endemic regions which also come under the low- or middle-income countries. For instance, in Nigeria, a complete dose of quinine for a seven-day course costs about $1.2 (₦ 840), while a 3-day treatment using artemether/ lumefantrine (Coartem®) costs about $2.5 (₦ 1,800). Artemisinin-based combination therapy (ACT) which has become the mainstay for the treatment of uncomplicated malaria, is bedevilled with challenges including development of resistance and high cost of purchase in resource-limited settings. Less than 50 years after its discovery in the 1970's, artemisinin resistance was first reported in 2009. Since then, a good number reports have continued to surface of malaria parasite resistance to artemisinins [4]. There is rising fears that if nothing drastic is done in terms of discovery of potent therapies for malaria or repurposing of existing drugs, malaria may become a pandemic again. Hence our research was aimed at redesigning quinine and investigating an alternative route for its administration for the treatment of malaria. To the best of our knowledge, no research investigating the intranasal administration of quinine for the treatment of malaria has been published. However, quinine nasal spray is being investigated for prevention of infection by SARS-CoV-2 virus [5].

A nanosuspension of quinine was formulated to suit intranasal administration. The nasal cavity is highly vascularized with a relatively large surface area (96 m^2), making it an attractive route for drug administration [6]. Therefore, this route of drug administration can be exploited for drugs such as quinine which are beset with numerous GIT side effects. This may be beneficial in handling some of the side effects of quinine that are due to systemic exposure. The relatively reduced surface area

of the nasal cavity compared to the GIT may reduce the rate of saturation of the systemic circulation with quinine, thereby preventing side effects such as cinchonism which is dependent on the concentration of quinine in circulation[7]. The intranasal route also offers the advantage of ease of application and painless self-administration, just like the oral route. However, unlike the oral route, drugs administered through this route can avoid first-pass metabolism, as well as achieve direct brain access through the olfactory region [8]. Besides, a previous study targeting quinine to the brain, with the aim of reducing serum concentration, toxity and improving efficacy in treatment of cerebral malaria has been reported [9]. Other side effects that may be avoided by administring quinine through the nasal route include hypotension (which may occur when the drug is given too rapidily, e.g. through intravenous injection), venous thrombosis (this is usual with intravous administration), pain and sterile abcessess at the site of injection (which happens when intramuscularly administered) [1]. The rectal route is yet another route which may offer a slower administration of quinine, in addition to avoidance of GIT exposure, however, a negative cultural perception of the rectal route may limit its use [10].

Nanotechnology is yet another means that has been employed for the revival of drugs and enhancement of the their therapeutic potentials, in addition to the reduction of side effect profiles [11]. A good number of anitparasitic drugs such as halofantrine, primaquine, atovaquone as well as quinine [12] has been prepared as nanoformulations in order to improve drug solubility, enhance drug release, and achieve specific drug targeting. Designing of quinine as nanocapsule was found to increase interaction between quinine and the erythrocyte, resulting in an increase in its *in vivo* efficacy in malaria infected rats[12]. It is based on this premise that a nanosuspension of quinine was designed to suite intransal administration.

In this present study, the ability of the redesigned and rerouted quinine to treat malaria was investigated by formulating nanosuspension of quinine using different lipids, characterization of NS was performed, after which QHCl-Ns were administered intranasally to mice infected with *Plasmodiumberghei* ANKA. Results obtained were compared with orally adminitered quinine and plain unprocessed quinine solution.

2. Materials And Methods

Materials

QHCl (purity ≥ 95 %) was obtained from Sigma-Aldrich (England, UK). Softisan® 154 (S154) and Miglyol® 812 N (Medium chain triglycerides (MCT)) were gifts from IOI Oleo GmbH, (Witten, Germany). Compritol® 888 ATO (C888) (Glycerol dibehenate), Compritol® HD 5 ATO (CHD 5) (Behenoyl polyoxyl-8 glycerides) and Transcutol® HP (THP) (Diethylene glycol monoethyl ether) were also gifts from Gattefossé SAS (Saint-Priest Cedex, France). Free samples of Phospholipon® 90H (P90H) were obtained from Lipoid GmbH (Ludwigshafen, Germany). Stearic acid, Poloxamer® 188 (P188) and Tween® 80 (T80) were purchased from Sigma-Aldrich (England, UK). Ultrapure water was sourced from ELGA Purelab Ultra Genetic Water Purification System (UK). All other reagents were of analytical grade and purchased from standard commercial suppliers.

Methods

2.1 Determination of QHCl solubility in solid and liquid lipids

The solubilities QHCl in solid lipids (stearic acid, S154, CHD 5 and C888) as well as liquid lipids (Miglyol® 812 N and glyceryl monooleate) and the solvent, (Transcutol® HP) were determined using a modified version of the shake flask technique [13]. A 1:2 and 1:3 (w/w) ratio of the drug to lipid were prepared in each case and vortexed for 2 min. For the solid lipids, drugs were added to melted lipid (after15 min heating at 10 °C above their melting temperatures).The solid and lipid liquid were selected for the formulation based on the transparency of the drug-lipid mixture [13].

2.2 Formulation of SRMS lipid matrices

The SRMS lipid matrices consisting of 1:2 (30:70) mixtures of P90H and either of the lipids: S154, or CHD 5, or C888, were prepared by fusion method [14]. Each of the lipids and P90H were weighed using an electronic balance (Mettler Toledo - X A204

Delta range), melted together on a hot plate (BioCote® Stuart Hotplate stirrer) at 70 ºC and stirred with the help of a magnetic bead at 200 rpm. The temperature was reduced to room temperature after melting and mixing was completed to allow for solidification of lipid matrices. These were gently scraped out of the beakers and stored in air tight glass bottles.

2.3 Preparation of QHCl -NS

QHCl-loaded NS were prepared by combined ultrasonication technique, first with a cup-horn sonicator, and then a probe sonicator [8]. SRMS lipid matrix (3%) and MCT served as the solid and liquid lipid, respectively, while T80 (2, 3 or 5 %) was the surfactant. P188 (1%) and sorbitol (5 %) served as the stabilizer and cryoprotectant, respectively. First, melting of the solid lipid was done at 70 °C on a magnetic hot plate (BioCote® Stuart Hotplate stirrer), subsequently QHCl was dissolved in a mixture of THP and MCT and then added to the melted solid lipid matrix and mixed thoroughly at 300 rpm. An aqueous surfactant solution was added to the melted oil phase in drops with the help of a burette [15]. The aqueous surfactant solution contained T80, P188 and sorbitol and was heated to the same temperature as the lipid phase. Mixing of the two phases was carried out briefly on a magnetic stirrer at 70°C before sonication was performed in a cup-horn sonicator for 30, 60 or 90 min at 100 amp at 43 °C. Additional sonication was achieved with a probe sonicator for 3 min at 70 °. The same procedure was repeated for NS containing no drug (blanks), which served as placebos. All NS dispersions were divided into two, one part was freeze-dried (Labconco FreeZone 6 Plus, Kanas city, Missouri, USA) at -80 °C and at a pressure of 0.01 mmHg, while the other portion was used for some characterizations and stability studies. The compositions of QHCl -NS, and cup-horn sonication times of different formulations are stated in Table 1.

Table 1. Quantities of materials used for the formulation of QHCl -NS

QHCl - NS	Lipid Type	Concentration (%)							Cup-horn sonication time (min)
		QHCl	Solid lipid	MCT	THP	T80	P188	Sorbitol	
Q1	S154	1.5	3	1.5	1.5	3	1	5	30
Q3	S154	1.5	3	1.5	1.5	3	1	5	90
Q9	S154	1.5	3	1.5	1.5	2	1	5	60
Q10	S154	1.5	3	1.5	1.5	5	1	5	60
Q13	CHD 5	1.5	3	1.5	1.5	3	1	5	60
Q14	CHD 5	1.5	3	1.5	1.5	3	1	5	60
Q15	CHD 5	1.5	3	1.5	1.5	3	1	5	60
Q5	CHD 5	1.5	3	1.5	1.5	2	1	5	30
Q6	CHD 5	1.5	3	1.5	1.5	5	1	5	30
Q7	CHD 5	1.5	3	1.5	1.5	2	1	5	90
Q8	CHD 5	1.5	3	1.5	1.5	5	1	5	90
Q2	C888	1.5	3	1.5	1.5	3	1	5	30
Q4	C888	1.5	3	1.5	1.5	3	1	5	90
Q11	C888	1.5	3	1.5	1.5	2	1	5	60
Q12	C888	1.5	3	1.5	1.5	5	1	5	60

2.4 Characterization of QHCl -NS

2.4.1 Determination of particle sizes, polydispersity indices and zeta (ζ) potentials of NS

Particle size, polydispersity indices and zeta potential determination was done using a nanosizer (Malvern-Zetasizer Nano series, United Kingdom) immediately after formulation, as well as 30 and 90 days post formulation. Determination was carried out at 25 °C after dilution and three replicates were obtained for each measurement. Data is presented as mean ± standard deviation (SD) [16].

2.4.2 Determination of the morphology of QHCl -NS

2.4.2.1 Transmission electron microscopy (TEM) of QHCl

A transmission electron microscope (JEOL JEM-1400 USA, Inc.) was used in the determination of the morphology of the QHCl -NS. Appropriate dilution of QHCl-NS (a100 µl volume of each preparation diluted to 30 ml) using deionized water was done before placing NS on a 300-mesh carbon coated copper grid (FC300Cu, Formvar/Carbon film on Copper). A drying time of two minutes was allowed to enable NS to adhere to the carbon substrate. Negative staining with 2% uranyl acetate and subsequent air drying at room temperature for 1 min was carried out before observation was performed using TEM at 300 k magnification.

2.4.2.2 Cryo-scanning electron microscopy (cryo-SEM) and field emission SEM (FESEM) of NS

Morphological characterization was also done using cryo-SEM and field emission SEM. A drop of appropriately diluted QHCl-NS was placed on metal stubs and rapidly frozen with slush nitrogen until -210 °C and sublimated at -90 °C for 90 seconds. Coating was achieved with palladium under vacuum, and samples were fractured, transferred to the chamber, and examined using FESEM (Philips XL30 FEG ESEM). The observations were done at -150 °C [17], while micrographs were obtained at accelerated voltage of 5 kV at a pressure of 0.6 mmHg [18]. Morphology of dry samples (such as excipients, pure drug samples of quinine as well as freeze dried NS) was carried out using normal FESEM. Samples were places on double sided tapes stuck to an aluminium stud. The samples were coated for three minutes with gold using a sputter coater (EMS 7620 Mini Sputter Coater/Glow Discharge System) with deposition control adjusted to 25 mA. Afterwards, the coated samples were loaded into FESEM (Philips XL30 FEG ESEM) and micrographs were obtained at accelerated voltage of 15 kV, at a pressure of 0.6 mmHg [16].

2.4.3 Fourier transform infra-red (FTIR) spectroscopic analysis

Fourier transform infrared spectroscopy (ATR-FTIR) analysis of freeze-dried QHCl-NS and excipients was performed on a PerkinElmer Spectrum fitted with a universal ATR sampling accessory and recorded in the range of 4000 to 650 cm-1 at ambient temperature. Evaluations were performed using a 16 scan per sample cycle and a fixed universal compression force of 80N. Subsequent analyses were carried out using spectrum software [14,19].

2.4.4 Thermal analysis

Thermal analyses of freeze-dried samples of QHCl-NS, drug, physical mixtures of lipids and drug and other excipients were conducted using differential scanning calorimeter (DSC) (TA Instruments, DSC-25, U.K.). Samples were weighed into aluminium pans, hermetically sealed and determinations were performed at a heating rate of 10 °C/min over a temperature range of 10 – 200 °C under nitrogen purge at a flow rate of 80 cm3/min. Data analyses, and determination of melting points and enthalpies was done using TA Rheology Data Analysis software (TA Instruments Trios Version 4.1.33073, UK [20].

2.4.5 Powder X-ray diffractometry (XRD)

XRD patterns of drugs, excipients and QHCl-NS were obtained using a diffractometer (SIEMENS/BRUKER D5005, Munich, Germany). The samples were exposed to Cu Kα radiation (40 kV, 35 mA) and measurements were carried out at room temperature. Scanning was carried out at 2θ from 5° to 90°, for 30 min (for excipients) or 1 h (for NS) [8].

2.4.6 Time-dependent pH stability studies of NS

pH of QHL-NS as well as blanks were analysed in triplicates, and at room temperature on day 1, 30, and 90 using a pH meter (pHep® Hana Instruments, Italy) [21].

2.4.7 Osmolality determination

Osmolality of NS were determined using an Osmometer (OSMOMAT 3000, Gonotec, Germany). A 100 µl quantity of each formulation was used, and the average of three determinations was obtained [22].

2.5 Solubility analysis of QHCl in simulated nasal fluid and alcoholic buffer

A concentration above expected solubility level of QHCl (8%) was prepared in simulated nasal fluid (SNF) (8.77 g NaCl, 2.98 g KCl and 0.59 g CaCl2 per 1000 ml of demineralised water, pH of 6.4). Suspensions were kept in an incubator/shaker (Multitron Infors HT, Bottmingen, Switzerland) maintained at 37± 0.5 °C with continuous stirring at 100 rpm. After 24 h, samples were carefully withdrawn and filtered through 0.45-µm nylon syringe filters, diluted 1000 times and analysed using HPLC [23].

2.6 *In vitro* release studies of QHCl-NS

Release studies were conducted in SNF. Amounts of freeze-dried QHCl-NS containing 5 mg of the drugs were placed in polycarbonated dialysis membrane (length: 6 cm, pore size: 2.4 nm, molecular weight cut off: 12 000 – 14 000 Da) which was previously soaked overnight in distilled water prior to the procedure, and immersed in 100 ml of release media. The set-up was maintained at 37 ± 0.5 °C and stirred at 60 rpm for a 24 h. At pre-determined time intervals, 1 ml portion of the dissolution media was withdrawn for HPLC analysis and replaced with 1 ml fresh medium. The amount of drug released at each time point was calculated with reference to the relevant calibration plot. In vitro analyses of pure QHCl were also carried out following the same method. Each procedure was performed in triplicate. Kinetic evaluation of release profiles was done by fitting the data into zero-order, first-order and Higuchi square-root models [15]. Korsmeyer-Peppas equation was also taken into consideration for determination of the release mechanism [24]. For Korsmeyer-Peppas model, only the data points with less than 60 % release was used for model fitting [25].

2.7 *Ex vivo* permeation studies of QHCl-NS

Franz diffusion cells were used for the determination of the permeation efficacy of QHCl-loaded NS across porcine nasal mucosa from one selected formulation (Q9). Diffusion cells with surface area of 6.6 cm^2 and volume of 10 ml were used. Appropriate volumes of deaerated SNF (pH 6.4) was placed in each of the Franz diffusion cells and allowed to equilibrate at 37 ± 0.5 °C for 15 min on a heated magnetic block. Fresh nasal pig tissue was obtained at the local slaughter house with prior permission from concerned authorities at the abattoir. Moreover, all animal experimental protocols were carried out in accordance with guidelines of the Animal Ethics Committee of the University of Nigeria, Nsukka and EU Directive 2010/63/EU for animal experiments. The nasal mucosa was detached from the septum, connective and cartilaginous tissues and stored in phosphate buffered saline (pH 6.4) during transportation. During each procedure, the nasal mucosa was individually placed on the Franz diffusion cells and clamped between the donor and receptor compartments, and sealed with paraffin to prevent loss of moisture during the 3 h period. Before sealing was done, amounts of Q9 NS containing 0.5 mg of QHCl, was placed on the membrane surface on the donor compartment and stirring was done at 600 rpm. A gel-loading pipette tip attached to a micro-pipette was used to withdraw 600 µl of the media from the receptor compartment at pre-determined time intervals and replaced with the same volume of fresh SNF [15,26]. Permeation of pure unprocessed QHCl were also carried out to serve as positive control, The results obtained were used to construct a permeation profile by plotting the amount of drug permeated per unit surface area (mg/cm2) versus time (min). The steady state flux (Jss, mg/cm^2 min) was calculated from the slope of the plot using linear regression analysis [8].

The drug apparent permeability coefficient (Papp) was calculated according to the equation:

$$Papp = \frac{dQ}{dt} \times \frac{1}{A.C_0.60} \quad (1)$$

where Papp is the apparent permeability coefficient (cm/s), dQ/dt is the cumulative amount of drug permeated vs. time per unit area (flux), A is the effective surface area (cm^2) and Co is the initial concentration ($\mu g/cm^3$).

2.8 *In vivo* pharmacodynamic studies

The guidelines of the Animal Ethics Committee of the University of Nigeria, Nsukka and EU Directive 2010/63/EU were observed while conducting the *in vivo* pharmacodynamic studies in mice. CBA/J mice, weighing 18 – 20 g were made to develop malaria by intraperitoneal inoculation of 2 x 10^5 *Plasmodium berghei* ANKA parasitized erythrocytes from a previously infected mouse [27,28]. Grouping into 5 sets of 6 was done on day seven (7) post-infection as shown on Table 2. Table 2 also shows the treatments administered, doses as well as routes of administration.

Table 2. Treatments administered in *in vivo* studies

Formulation/API	Group	Treatment	Dosing	Route
QHCl	Q1	Q9	20 mg/kg at 0 h,	IN
	Q2	Plain QHCl solution	10 mg/kg every 12 h for 4 days	
	Q3	Q9		Oral
Placebo	Q4	Blank NS	20 mg/kg at 0 h,	IN
	Q5		10 mg/kg every 12 h for 4 days	Oral

Mice receiving treatment intranasally were slightly anesthetized using ketamine at a dose of 75 mg/kg. To administer NS intranasally, each mouse was held using the left hand and restrained by anchoring tail between the small finger and the palm [29,30], after which the mice were held in a supine position with the head elevated. Using the right hand, gel loading tips attached to a micropipette were used to slowly introduce the right dose of each formulation through the external nares. Dose volumes were adjusted to ≤ 20 µl to avoid suffocation and death [31,32]. Mice were maintained in standing position until they recovered from the effect of the anaesthesia. On day 13 post infection each mouse was tail-bled and a thin blood film was made on a microscope slide. The films were fixed with methanol, stained with gentian violet solution and examined microscopically to monitor the parasitaemia level. Level of parasitaemia at day 1 post infection was used for comparison.

Percentage of parasitaemia in the blood was calculated using the expression:

$$\%\ \text{Reduction in Parasitaemia} = 100 - \{\text{No. of parasitized RBC}/(\text{No. of parasitized RBC} + \text{No. of nonparasitized RBC})\} \times 100 \quad (2)$$

Antimalarial activity of formulations and pure drug was determined by using the equation:

$$\text{Activity}\ (\%) = 100 - \left(\frac{\text{Mean parasitaemia in treated group}}{\text{Mean parasitaemia in control group}}\right) \times 100 \quad (3)$$

*RBC (Red blood cell count).

2.9 Histopathological studies

After intranasal administration with Q9 NS, mice were sacrificed by cervical dislocation. Histopathological examination of samples collected from the nasal mucosa and lungs was conducted after samples were fixed with 10 % neutral-buffered formalin and dehydrated in graded concentrations of ethanol. Samples were subsequently cleared in xylene and embedded in paraffin wax. Exactly 5 µm thick sections of the samples were cut and mounted on glass slide, and later stained with hematoxylin and eosin (H & E). Photomicrographs of sections were captured using Moticam Images Plus 2.0 digital camera (Motic China Group Ltd.) attached to a Leica binocular light microscope [33].

2.10 Data and statistical analysis

Results were expressed as mean ± standard deviation. For group comparisons, statistically significant differences were determined at $p < 0.05$ using one-way analysis of variance. Statistical analyses were done using GraphPad Prism version 8.2.0 (Prisma, Graphpad Software, La Jolla, US) [34].

3. Results And Discussion

3.1 Solubility of QHCl in solid lipids and liquid lipids

Since the solubility of any drug [especially hydrophilic drugs like QHCl] is crucial in any lipid-based drug delivery system, the solubility of QHCl was analysed in selected solid and liquid lipids. Of all the solid lipids analysed, CHD 5 was a better solvent for QHCl, with stearic acid showing lest solubility (Table 3). Solubilization of QHCl in stearic acid was only possible after heating was carried out at 80 °C for up to 15 min. The Compritol® lipids (CHD 5 and C888) and S154 were selected for the preparation of NS because QHCl was better solubilized in them and at lower temperatures. On the other hand, after the solubility test, QHCl was significantly dissolved in all the liquid lipids tested, with THP exhibiting the highest solubility. Hence, THP and Miglyol® 812 N were selected to serve as the co-solvent and liquid lipid, respectively. Transcutol® HP, the highest purity grade of diethylene glycol monoethyl ether has been known to exhibit good solubility for poorly soluble drugs like risperidone [35] due to the presence of an ether and an alcohol function groups in its molecule [36]. It is therefore used as co-solvent, surfactant e.t.c. THP was also selected for use in this intranasal formulation due to its skin permeation enhancement property [37]. Despite its high solubility, it could not be used alone as solvent, because it is toxic at high concentrations [38].

Table 3. Solubility of QHCl in solid and liquid lipids

Solid Lipids	**Stearic acid**	**Softisan® 154**	**Compritol® HD 5 ATO**	**Compritol® 888 ATO**
QHCl Solubility	+	++	+++	++
Liquid Lipids	**Miglyol® 812 N**	**Glyceryl monooleate**	**Transcutol® HP**	
QHCl Solubility	+++	+++	++++	
Key: + = Sparingly soluble; ++ = Slightly soluble; +++ = Soluble; ++++ = Freely soluble, - = not soluble				

3.2 Mean particle size and Particle Distribution Indices analyses of QHCl-NS

Even though CHD 5 produced a higher solubility of QHCl, lipid matrices made with C888 and S154 were also used in the formulation of NS. In addition, three concentrations of surfactant and different sonication times were employed to determine the effect of varying these process parameters on average particle sizes and PDI of NS. All QHCl-NS had mean particles in the nanometer size range (68.6±0.86 to 300.8±10.11 nm) (Table 4, Fig. 1).

Table 4. Particle size (24 h, 30 and 90days), PDI and Zeta potential of QHCl-NS

QHCl-NS	24 h			30 days		90 days	
	Particle size (nm)	PDI	Zeta Potential	Particle size (nm)	PDI	Particle size (nm)	PDI
Q1	194.76±4.495	0.441±0.006	6.72±0.259	199.27±0.4225	0.433±0.011	192.1±2.371	0.427±0.013
Q3	118.4±0.7216	0.426±0.017	3.24±0.304	143.4±0.6202	0.406±0.2646	177.0±3.704	0.237±0.016
Q9	117.5±1.53	0.282±0.004	6.95±0.416	112.2±1.715	0.279±0.004	113.7±0.7550	0.279±0.007
Q10	80.9±1.57	0.465±0.015	4.74±0.371	68.15±0.8786	0.456±0.003	60.85±0.5901	0.442±0.013
Q13	92.9±2.765	0.564±0.032	4.81±0.067	97.51±0.767	0.431±0.029	90.58±0.747	0.315±0.003
Q14	109.4±0.814	0.599±0.011	4.92±0.096	115.2±0.7092	0.443±0.005	130.2±0.4173	0.211±0.011
Q15	120.5±4.828	0.574±0.027	4.28±0.180	97.67±1.640	0.425±0.015	104.2±0.7024	0.280±0.003
Q5	83.52±0.676	0.467±0.008	6.19±0.396	86.92±0.999	0.319±0.020	92.82±0.5046	0.255±0.010
Q6	150±1.595	0.475±0.007	5.36±0.106	120.5±0.808	0.371±0.006	130.8±0.625	0.268±0.005
Q7	68.6±0.861	0.491±0.003	5.93±0.18	79.9±2.87	0.261±0.010	87.31±1.160	0.225±0.005
Q8	90.36±0.520	0.445±0.003	4.36±0.076	90.50±2.859	0.307±0.028	97.51±0.197	0.307±0.028
Q2	300.8±10.11	0.603±0.029	4.23±0.294	206±27.97	0.596±0.146	186.9±16.12	0.557±0.073
Q4	121.5±39.62	0.397±0.132	2.31±0.061	121.5±39.62	0.397±0.132	143.3±1.739	0.441±0.012
Q11	119.4±0.945	0.511±0.008	0.738±0.138	109.1±1.649	0.488±0.006	113.2±4.192	0.475±0.017
Q12	118.6±1.093	0.492±0.022	2.16±0.659	103.5±1.580	0.434±0.007	111.8±4.925	0.318±0.037

In all the lipid matrices used, increasing sonication time from 30 to 90 minutes did better at reducing particle size than increasing surfactant concentration from 2 to 5 %. In the case of QHCl-NS made with CHD 5 and C888, increasing concentration of surfactant resulted instead in an increase in particle size (compare Q5 and Q7, and Q6 and Q8, Fig. 2). Hence, it can be concluded that it is not in all cases that increasing concentration of surfactant will result in reduction in particle sizes [39].Increasing surfactant concentration may produce smaller particle sizes than increasing sonication time, especially when the concentration of the liquid lipid is high [8]. NS formulated with S154 produced more predictable results in terms of the particle sizes of QHCl-NS. Increasing sonication or surfactant resulted in reduction of particle sizes, even though increasing sonication time still yielded smaller particle size better than using higher concentration of surfactant (Q1 compared with Q3, and Q9 compared with 10, Table 4).

The differences observed in the particle sizes of the QHCl-NS made from the three lipid matrices can be attributed to their constituents and characteristics, S154 is hydrogenated palm oil made up of C14-C18 fatty acids and has a melting point of approximately 55 °C [40], while C888 is docosanoic acid, monoester with glycerine, having a melting point of 69-74 °C. In addition to the constituents of C888, CHD 5 also contains poly(ethylene)glycol and melts at a lower temperature (56-63 °C) [41,42].

The PDIs of QHCl-NS formulations were in the range of 0.282±0.004 to 0.603±0.029 immediately after formulation, and the PDI of QHCl-NS prepared with C888 (Q2, Q4 and Q11) were all significantly higher than NS prepared with CHD 5, and especially S154 (Table 4). It was observed that PDI increased with reduction in mean particle size. So that smaller particles had higher PDI than larger particles (compare Q9 with Q7 and Q10 on Table 4).

The nanosizes obtained may be beneficial to the usefulness of QHCl, since drugs in such sizes can access the brain through the olfactory region of the nasal cavity. It can also improve permeability through the nasal mucosa. Deductions made from the results on the influence of sonication of duration and concentration of surfactant shows that these parameters significantly

affect the final size of lipid nanoparticles. Therefore, preformulation studies to monitor average particle size while varying these parameters must be performed in order to determine the optimal conditions that would yield monodispersed, nano-sized lipid particles.

3.2.1 90 days Stability studies of QHCl-NS

The QHCl-NS formulated were very stable. Only 6 formulations out of 12 increased in size (negligibly) after 1 month. In some cases, a reduction in size and PDI was recorded (Table 4). This has been reported by other researchers [8,43,44] and is caused by loss of solubilized water situated within the core of the nanoformulation. It may still be due to the ultrasonic energy used for size reduction which is known to cause collision of smaller oil droplets to form large ones [45,46], a phenomenon termed "sonication induced aggregate formation"[13,47]. Removal of the ultrasonic energy during storage may have led to a stable system resulting to reduction in particle size and PDI.

The high stability of the QHCl-NS formulation may be due to the surfactant (T80) and stabilizer use (P188) during formulation.

3.2.2 Surface charge (Zeta (ζ) potential) of NS

The low zeta potential values recorded for QHCl-NS (0.738±0.138 to 6.72±0.259 mV) is attributed to the use of non-ionic surfactants (T80 and P188) (Tables 4 and Table S1) [48]. The zeta potential of blank formulations was higher than that of the drug containing NS (Table S1). All QHCl-NS were positively charged within the first 24 h after preparation, however, some C888 containing formulations became slightly negatively charged after 30 and 90 days of storage. The low zeta potential did not cause increase in sizes of nanoparticles on storage. This stability in sizes on storage may be due to the presence of P188 which is known to cause steric stabilization [49,50] .

Three QHCl-NS formulations (Q7, Q9 and Q12) representing the three lipid matrices used (CHD 5, S154 and C888, respectively) were selected for further characterizations based on their acceptable particle sizes, PDI and high stability during storage.

3.3 Time-dependent pH stability studies and Osmolality of QHCl-NS

pH of QHCl-NS formulations (5.03-5.55) were within the acceptable pH range for nasal formulations (pH of 4.5 to 6.5) [51], and remained stable for 90 days while being stored at 8±2 °C (Fig. 3). Osmolality of the formulations ranged from 422.3 ± 12.3 to 517.0 ± 21.7 mOsmol/kg (Table 5), which is within range of most marketed nasal products (300 – 700 mOsmol/kg) [52]. Therefore, nasal irritation due to pH disparity or tonicity is unlikely to occur during administration.

Table 5. Osmolality, ex vivo permeation results and drug release mechanism and kinetics of QHCl-NS

Batches	Osmolality (mOsmol/kg)	Flux (μg/cm^{2}min)	Permeation coefficient (cm/sec)	Zero Order	First Order	Higuchi	Korsmeyer-Peppas	
				r^2	r^2	r^2	r^2	n
Q7	422.3 ± 12.3	-	-	0.7807	0.9161	0.9939	0.9756	0.5055
Q9	492.7 ± 17.9	320.710	2.18×10^{-2}	0.7466	0.8885	0.9298	0.9993	0.8869
Q12	517.0 ± 21.7	-	-	0.8603	0.9611	0.9710	1	0.7730
Plain Solution of QHCl	-	56.973	3.87×10^{-4}	-	-	-	-	-

3.4 Morphology of QHCl-NS

The photomicrograph obtained from both TEM and SEM revealed round and oval-shaped NS particles (Fig 4A-D). During our experiments, we observed that cryo-SEM was a better method for visualizing NS compared to SEM. Cryo-SEM was able to reveal

more distinct particles. The images obtained from SEM was clumped together, making visualization of individual particles difficult (Fig. 4 C&D). This difference may have been caused by lyophilization, since the samples used in SEM were lyophilized solid samples, while NS formulations in liquid form were used for cryo-SEM analysis. The photomicrographs of excipients and other NS formulations are presented in Fig. S2.

3.5 FTIR spectroscopic analysis

Fourier transform infra-red spectrophotometer was used to determine possible interactions between the constituents of the lipid matrix (Softisan® 154, Compritol® HD 5 ATO and Compritol® 888 ATO, and Phospholipon® 90H) and between the lipid matrix and drug. The lipids (S154, CHD 5 and C888) were compatible with the P90H, as revealed in the FTIR spectra of the lipid matrices (Fig. S3). The same principal peaks were evident in the FTIR spectra of the individual lipids and phospholipid as in the spectra of the lipid matrices. This suggests that the use of heat in the fusion of P90H and the lipids did not result in a chemical interaction.

In addition, FTIR results confirmed the lack of chemical interaction and compatibility of QHCl with the lipid matrices used as well as other excipients. Apart from the broadening and shortening of some principal peaks in the FTIR spectra of the selected formulations (Fig. S3), no other difference was noticed. This difference may be attributed to hydrogen bond interactions as well as the presence of other excipients [24]. Hence, designing of QHCl as nanosuspension did not alter the chemistry of the drug, and it is expected not to loss its antimalaria activity.

3.6 Crystalline state of QHCl-NS

DSC analysis was conducted for unprocessed QHCl, excipients and physical mixtures of the drug and lipids. All the solid lipids were crystalline in nature (sharp melting endothermic peaks at 57.68, 72.53 and 59.56 °C, enthalpies of 94.675, 116.25 and 117.83 J/g for pure S154, C888 and CHD5, respectively (Table S2)). P90H also showed an endothermic peak (122.30 °C). Fusion of the solid lipids with P90H during the formation of the SRMS caused reductions in melting points and enthalpies (Table S2). A complete disappearance of the melting peak due to P90H with the fusion of C888 and P90H implied that P90H was completely molecularly dispersed or amorphous in C888 (Fig. S4) [53]. On the other hand, the inclusion of the liquid lipid (MCT) also caused further depression in the melting points of all solid lipid matrices, and so did the addition of Transcutol® HP (Table S2). The reduction of the melting points of solid lipids in the presence of liquid lipids and drugs has been previously reported by Garcia-Fuentes et al. [54] and Hu et al. [55]. Le-Jiao and co-authors [56] also reported a decrease in enthalpies of nanostructured lipid carriers with the addition of MCT. This is defined as a eutectic behaviour [53] and suggests a disordered lattice that can accommodate more drug molecules[8].

The melting point and enthalpy of unprocessed QHCl (117.29 °C) reduced when formulated as NS (57.11, 56.29 and 63.63 °C, for Q7, Q9 and Q12 respectively) suggesting amorphization (Fig. 5). However, this was further investigated using X-ray diffractometry, because it may be erroneous to conclude on the crystal nature of a drug using DSC when it is available in low concentrations (less than 10 %).

3.7 Powder X-ray diffractometry of NS

X-ray diffractograms of QHCl-NS confirmed a reduction in crystallinity, since there were disappearances of some peaks in the diffractogram of the NS, unlike in the unprocessed drug (Fig. 6A-D). For instance, some peaks in unprocessed QHCl at 2θ of 10° to 20° (Fig. 6A) were not seen in Q7 (Figs. 6B), while peaks at 2θ of 13.4° and 24.0° in pure QHCl were lost in Q9 (Figs. 6C). Also, so many sharp peaks were not visible in Q12 (Figs. 6D) compared to the pure quinine hydrochloride. For example, sharp distinct peaks at 2θ of 9.2°, 14.6°, 17.9° and 23.9°to 48.9° in pure quinine sample were not detected in Q12 (Figs. 6D). Amorphous halos were also very visible on the XRD patterns of the NS, an indication of the presence of some amorphous form of the drug. It can therefore be concluded that QHCl were in microcrystalline or semi-crystalline form in the NS [57,58].

3.8 In vitro release studies of QHCl-NS

3.8.1 *In vitro* release analysis of QHCl-NS

In vitro drug release was conducted in SNF in order to mimic the nasal environment. Solubility of QHCl in SNF was determined to be 26.49 mg/ml. Sink condition was maintained throughout the procedure by using a volume that will accommodate solubilized drug without saturation occurring, as well as by replenishing with fresh media after each withdrawal of samples for analyses. Neither concentration of surfactant nor particle size significantly influenced drug release among QHCl-loaded formulations (Fig. 7). This may have been due to high solubility of QHCl in the release media (26.49 mg/ml). Although pure unprocessed QHCl released slightly more drug than all the selected QHCl formulations (Q7, Q9, Q12), after the 6th hour, all formulations released above 80% of their drug content, with Q9 (formulated with S154) NS showing the fastest rate of release. The faster rate of release of pure unprocessed API compared to drugs in nanoformulations has been reported by other researches [25], and may be attributed to time required for the release media to by-pass the lipid carrier system wherein the drug is encapsulated or dispersed.

3.8.2 Evaluation of drug release mechanism and kinetics of QHCl-NS

Zero order, first order and Higuchi mathematical models were used to evaluate the kinetics of drug release from NS. The model that gave the highest correlation coefficient value was considered the best fit for the release data being analysed [24,59]. Drug release from all QHCl NS followed Higuchi release kinetics (Table 5). The mechanism of drug release was determined using Korsmeyer-Peppas model (Table 5). “n” value for Q7 was 0.5055 indicating a Fickian diffusion-controlled mechanism. Diffusion of quinine from Q9 and Q12 was by anomalous diffusion, implying that release of quinine from these NS formulations was by both diffusion and erosion of the lipid matrix since diffusional release exponent was greater than 0.5 but less than 1(Table 5).

3.9 Ex vivo Permeation analysis of QHC1-NS

The *ex vivo* permeation analysis and the *in vivo* antimalarial study was conducted using only Q9 because this formulation exhibited a higher *in vitro* release than the other selected formulations (Q7 and Q12). Results obtained were compared with the unprocessed QHCl to determine the effect of formulating quinine as NS. The flux and permeation coefficient of Q9 (320.71 $\mu g/cm^2 min$ and 2.18 x 10^{-2}cm/sec, respectively) were significantly ($p < 0.05$) higher than that of the unprocessed pure sample of QHCl (56.97 $\mu g/cm^2 min$ and 3.87 x 10^{-4}cm/sec, respectively) (Table 5). A 5-fold and 56- fold increase in flux and permeation coefficient, respectively was observed. This implies that the rate of absorption as well as ease of drug permeation through porcine nasal mucosa was impressively enhanced by formulating QHCl as NS. A similar outcome has been earlier reported for artesunate NLC and gentamicin lipid-based microsuspension [8,22]. The lipophilicity of NS improved the permeation of QHCl, a hydrophilic drug, through excised porcine nasal mucosa. This also implies that the reformulation of QHCl can improve its permeation through lipid bilayers.

3.10 In vivo antimalarial studies of QHCl NS

Antimalarial investigation showed that there was significant ($p < 0.05$) reduction of parasitaemia achieved with both intranasal and oral administration of QHCl-NS compared with placebo. Reduction in parasitaemia caused by Q9 administered through the intranasal and oral routes were 51.16 %, and 52.12 %, respectively (Fig. 8). Interestingly, reduction in parasitaemia observed in both routes of administration were similar and non-significantly different, though that of the oral route was higher. This is an indication that malaria treatment with quinine through the intranasal route is a possibility. The activity of the drug when given through the nasal route (56.26 %) was higher than when administered through the oral route (54.22%). Administration of unprocessed quinine solution exhibited significantly ($p < 0.05$) higher reduction in parasitaemia and activity. This varies from the results obtained in the *ex vivo* permeation studies. However, for the intranasal administration, an NS formulation of quinine will still be preferrable because such a formulation being mucoadhesive will be better retained in the nasal region [60]. A plain solution of the drug may easily be cleared in the nasal cavity, as well as run off to the oral region of the mouth or throat, causing the patient to experience an unpleasant taste.

3.11 Histopathological studies

The histopathological analysis of the lungs and the nasal mucosa showed a clear difference between the treated and the untreated groups. While there was evidence of inflammation and congestion of red blood cells in the in the lungs and nasal

mucosa of the mice in the untreated group (Fig. 10A and 11A) , none was observed in the lungs and nasal mucosa of mice treated intranasally with Q9 (Fig. 10B and 11B). The observed congestion of pulmonary vessels in the mice treated intranasally with placebo is indicative of severe malaria [61]. No sign of injury was seen in the group treated with Q9 through the intranasal route (Fig. 10B and 11B). However, the pseudo stratified columnar ciliated epithelium and non-ciliated goblet cells covered by thin mucus membrane were intact in both groups, and undamaged by intranasal administration of formulation and placebo. This implies that intranasal administration of NS formulation of QHCl for the treatment of malaria caused no damage to the nasal mucosa.

4. Conclusions

Intranasal administration of QHCl-NS successfully treated malaria in mice infected with *Plasmodium berghei* ANKA, and can therefore, serve as an alternative to other routes of administration of QHCl for the treatment of malaria. It can be beneficial in preventing the GIT- associated side effects caused by QHCl, and can be helpful to patients (especially pregnant woman) who may be having the side effect of vomiting due to morning sickness and malaria. The relatively reduced surface area of the nasal cavity compared to the GIT may reduce the rate of saturation of the systemic circulation with quinine, thereby preventing cinchonism which is dependent on the concentration of quinine in circulation. The intranasal route also offers the advantage of ease of application, painless self-administration, avoidance of first-pass metabolism, and direct access to the brain in the case of cerebral malaria. The results of the *ex vivo* studies revealed the potential of the nanosuspension of QHCl improving permeation through the nasal mucosa. Its bioadhesive nature compared to unprocessed QHCl solution will increase the residence time of the drug in the nasal cavity and retard flow of the bitter tasting drug to the oral cavity.

Further studies to compare parenteral administration of QHCl to intranasal administration, as well as quantification of the amount of drug in the brain relative to systemic circulation after intranasal administration will be conducted.

Declarations

Supplementary Materials: The following supporting information were provided: Table S1: zeta potentials of blank-NS formulations, Figure S1: SEM micrographs of drug and some excipients, Figure S2: FTIR Spectra of Excipients and QHCl-NS formulation, Table S*2*: DSC analysis results of plain drugs and, lipids and lipid matrices, Figure S3: DSC thermogram of lipid matrix made with C888 and P90H.

Author Contributions:

Conceptualization, Chinazom Agbo, Anthony Attama and Kenneth Ofokansi, Data curation, Chinazom Agbo and Timothy Ugwuanyi, Formal analysis, Chinazom Agbo and Joy Reginald-Opara, Funding acquisition, Chinazom Agbo, Paul Akpa, Christopher McConville, Anthony Attama and Kenneth Ofokansi, Investigation, Chinazom Agbo and Timothy Ugwuanyi, Methodology, Chinazom Agbo, Adaeze Onugwu, Adaeze Echezona, Chinekwu Nwagwu, John Ogbonna, Petra Nnamani, Lydia Ugorji, Christopher McConville, Anthony Attama and Kenneth Ofokansi, Project administration, Chinazom Agbo, Christopher McConville, Anthony Attama and Kenneth Ofokansi, Resources, Anthony Attama and Kenneth Ofokansi, Software, Chinazom Agbo, Supervision, Christopher McConville, Anthony Attama and Kenneth Ofokansi, Validation, Chinazom Agbo, Visualization, Chinazom Agbo, Timothy Ugwuanyi, Christopher McConville, Anthony Attama and Kenneth Ofokansi, Writing – original draft, Chinazom Agbo and Timothy Ugwuanyi, Writing – review & editing, Osita Eze, Adaeze Onugwu, Adaeze Echezona, Chinekwu Nwagwu, Samuel Uzondu and John Ogbonna.

Funding: The conducting of the research work was funded by the Commonwealth Scholarship Commission in the United Kingdom and African-German Network of Excellence in Science (AGNES), the Federal Ministry of Education and Research (BMBF) and the Alexender von Humboldt Foundation (AvH). The funders provided financial support but did not influence the study design, analysis and interpretation of data generated.

Institutional Review Board Statement: The study was conducted in accordance with the National Code of Conduct for Animal Research Ethics (NCARE). The animal study protocol was approved by the Animal Research Ethics Committee of University of

Nigeria, Nsukka (February. 7th, 2019.

Informed Consent Statement: Not applicable.

Data Availability Statement: Not applicable.

Acknowledgments:

We wish to thank the management of the University of Nigeria, Nsukka and University of Birmingham where this research was conducted. Our appreciation also goes to Lipoid GmbH and IOI Oleo GmbH for the gift of Phsopholipon® 90H, Softisan® 154, Compritol® 888 ATO, Compritol® HD5 ATO, Transcutol® HP, Transcutol® P and Miglyol® 812 N. Our sincere appreciation also goes to Offor Ejike, Nwabueze Harrison, Ubachukwu Ugochukwu, Ugwu Chinedu, Dr. Fredrick Ugwuoke, Gábor Drávavölgyi, Hanouf Bafhaid, Ali Al Amri, Sarah Lastakchi, Justyna Hofmanová and Sandya Rajesh for assisting in the laboratory procedures and the animal studies.

Conflicts of Interest: The authors declare no conflict of interest. The funders had no role in the design of the study, in the collection, analyses, or interpretation of data, in the writing of the manuscript, or in the decision to publish the results.

References

1. Achan, J., Talisuna, A.O., Erhart, A., Yeka, A., Tibenderana, J.K., Baliraine, F.N., Rosenthal, P.J., Alessandro, U.D. Quinine , an Old Anti-Malarial Drug in a Modern World : Role in the Treatment of Malaria. *Malar. J.* **2011**, *10*, 1–12.
2. World Health Organization *Guideline for the Treatment of Malaria, 3rd Edition*, 3rd ed., WHO Press, World Health Organization: Geneva, Switzerland, 2015,
3. Fairhurst, R.M., Wellems, T.E. Malaria (Plasmodium Species). In *Mandell Douglas, and Bennett's Principles and Practice of Infectious Diseases*, 2019, pp. 3070–3090.
4. Fairhurst, R.M., Dondrop, A.M. Artemisinin-Resistant Plasmodium Falciparum Malaria. *Microbiol. Spectr.* **2016**, *4*, 4–3.
5. U.S. National Library of Medicine GLS-1200 Topical Nasal Spray to Prevent SARS-CoV-2 Infection (COVID-19) Available online: https://clinicaltrials.gov/ct2/show/NCT04408183 (accessed on 31 August 2022).
6. Gizurarson, S. Anatomical and Histological Factors Affecting Intranasal Drug and Vaccine Delivery. *Curr. Drug Deliv.* **2012**, *9*, 566–582, doi:10.2174/156720112803529828.
7. Quinine. In *Meyler's Side Effects of Drugs*, Aronson, J.K., Ed., Elsevier: Oxford, 2016, pp. 27–35 ISBN 9780444537164.
8. Agbo, C.P., Ugwuanyi, T.C., Ugwuoke, W.I., McConville, C., Attama, A.A., Ofokansi, K.C. Intranasal Artesunate-Loaded Nanostructured Lipid Carriers: A Convenient Alternative to Parenteral Formulations for the Treatment of Severe and Cerebral Malaria - ScienceDirect. *J. Control. Release* **2021**, *334*, 224–236, doi:10.1016/j.jconrel.2021.04.020.
9. Gupta, Y., Jain, A., Jain, S.K. Transferrin-conjugated Solid Lipid Nanoparticles for Enhanced Delivery of Quinine Dihydrochloride to the Brain. *J. Pharm. Pharmacol.* **2007**, *59 (7),* 935–940.
10. Marijon, A., Bonnot, G., Fourier, A., Bringer, C., Lavoignat, A., Gagnieu, M.-C., Bienvenu, A.-L., Picot, S. Efficacy of Intranasal Administration of Artesunate in Experimental Cerebral Malaria. *Malar. J.* **2014**, *13*, 501, doi:10.1186/1475-2875-13-501.
11. Mumuni, M.A., Frankline, K.C., Ugwu, C.E., Musiliu, A.O., Agboke, A.A., Agbo, P., Ossai, E.C., Ofomata, A.C., Youngson, D.C., Omeje, C.E., et al. Development and Evaluation of Artemether-Loaded Microspheres Delivery System for Oral Application in Malaria Treatment. *Trop. J. Nat. Prod. Res.* **2021**, *5*, 2030–2036.
12. Haas, S.E., Bettoni, C.C., de Oliveira, L.K., Guterres, S.S., Costa, T.D. Nanoencapsulation Increases Quinine Antimalarial Efficacy against Plasmodium Berghei in Vivo. *Int. J. Antimicrob. Agents* **2009**, *34*, 156–161, doi:10.1016/J.IJANTIMICAG.2009.02.024.
13. Shah, B., Khunt, D., Bhatt, H., Misra, M., Padh, H. Application of Quality by Design Approach for Intranasal Delivery of Rivastigmine Loaded Solid Lipid Nanoparticles: Effect on Formulation and Characterization Parameters. *Eur. J. Pharm. Sci.* **2015**, *78*, 54–66, doi:10.1016/j.ejps.2015.07.002.

14. Agbo, C., Umeyor, C., Kenechukwu, F., Ogbonna, J., Chime, S., Lovelyn, C., Agubata, O., Ofokansi, K., Attama, A. Formulation Design, in Vitro Characterizations and Anti-Malarial Investigations of Artemether and Lumefantrine-Entrapped Solid Lipid Microparticles. *Drug Dev. Ind. Pharm.* **2016**, *42*, doi:10.3109/03639045.2016.1171331.
15. Jain, K., Sood, S., Gowthamarajan, K. Optimization of Artemether-Loaded NLC for Intranasal Delivery Using Central Composite Design. *Drug Deliv.* **2015**, doi:10.3109/10717544.2014.885999.
16. Gaba, B., Fazil, M., Khan, S., Ali, A., Baboota, S., Ali, J. Nanostructured Lipid Carrier System for Topical Delivery of Terbinafine Hydrochloride. *Bull. Fac. Pharmacy, Cairo Univ.* **2015**, *53*, 147–159, doi:10.1016/j.bfopcu.2015.10.001.
17. Tichota, D.M., Silva, A.C. Design , Characterization , and Clinical Evaluation of Argan Oil Nanostructured Lipid Carriers to Improve Skin Hydration. *Int. J. Nanomedicine* **2014**, *20*, 3855–3864.
18. Pretorius, E. Influence of Acceleration Voltage on Scanning Electron Microscopy of Human Blood Platelets. *Microsc. Res. Tech.* **2010**, *73*, 225–228, doi:doi.org/10.1002/jemt.20778.
19. Jiang, Y., Meng, X., Wu, Z., Qi, X. Modified Chitosan Thermosensitive Hydrogel Enables Sustained and Efficient Anti-Tumor Therapy via Intratumoral Injection. *Carbohydr. Polym.* **2016**, *144*, 245–253, doi:10.1016/j.carbpol.2016.02.059.
20. Mallappa, P., Prabirkumar, S., Panchakshari, A. Taste Masked Quinine Sulphate Loaded Solid Lipid Nanoparticles for Flexible Pediatric Dosing. **2014**, *48*, 93–99, doi:10.5530/ijper.48.4s.12.
21. Momoh, M.A., Franklin, K.C., Agbo, C.P., Ugwu, C.E., Adedokun, M.O., Anthony, O.C., Chidozie, O.E., Okorie, A.N. Microemulsion-Based Approach for Oral Delivery of Insulin: Formulation Design and Characterization. *Heliyon* **2020**, *6*, 1–8, doi:10.1016/j.heliyon.2020.e03650.
22. Onugwu, A.L., Agbo, C.P., Nwagwu, C.S., Uzondu, E., Echezona, A.C., Dike, J., Ogbonna, N., Akpa, P.A., Momoh, M.A., Nnamani, P.O., et al. Development of Lipid-Based Microsuspensions for Improved Ophthalmic Delivery of Gentamicin Sulphate. **2021**.
23. FDA *Dissolution Methods Database*, Washington, DC, USA, 2019,
24. Ümİt, G., Melİke, Ü., Gülgün, Y., Ecem Fatma, K., Aydoğmuş, Z. Formulation and Characterization of Solid Lipid Nanoparticles , Nanostructured Lipid Carriers and Nanoemulsion of Lornoxicam for Transdermal Delivery. *Acta Pharm* **2015**, *65*, 1–13, doi:10.1515/acph-2015-0009.
25. Weng, J., Tong, H.H.Y., Chow, S.F. In Vitro Release Study of the Polymeric Drug Nanoparticles: Development and Validation of a Novel Method. *Pharmaceutics* **2020**, *12*, 1–18, doi:10.3390/pharmaceutics12080732.
26. Ng, S.F., Rouse, J., Sanderson, D., Eccleston, G. A Comparative Study of Transmembrane Diffusion and Permeation of Ibuprofen across Synthetic Membranes Using Franz Diffusion Cells. *Pharmaceutics* **2010**, doi:10.3390/pharmaceutics2020209.
27. Clemmer, L., Martins, Y.C., Zanini, G.M., Frangos, J.A., Carvalho, L.J.M. Artemether and Artesunate Show the Highest Efficacies in Rescuing Mice with Late-Stage Cerebral Malaria and Rapidly Decrease Leukocyte Accumulation in the Brain. *Antimicrob. Agents Chemother.* **2011**, *55*, 1383–1390, doi:10.1128/AAC.01277-10.
28. Craig, A.G., Grau, G.E., Janse, C., Kazura, J.W., Milner, D., Barnwell, J.W., Turner, G., Langhorne, J., Malaria", on behalf of the participants of the H.R. meeting on "Animal M. for R. on S. The Role of Animal Models for Research on Severe Malaria. *PLoS Pathog.* **2012**, *8*, e1002401, doi:10.1371/journal.ppat.1002401.
29. Shimizu, S. Routes of Administration. In *The Laboratory Mouse (Handbook of Experimental Animals) - USP*, Tsukuba, 2004, pp. 527–541 ISBN 0123364256.
30. Simmons, M.L., Brick, J.O. *The Laboratory Mouse*, Hollaender, A., Ed., Prentice-Hall Inc., Englewood Cliffs., 1970,
31. Shen, X., Lagergård, T., Yang, Y., Lindblad, M., Fredriksson, M., Holmgren, J.A.N., Mmun, I.N.I. Group B Streptococcus Capsular Polysaccharide-Cholera Toxin B Subunit Conjugate Vaccines Prepared by Different Methods for Intranasal Immunization. *Infect. Immun.* **2001**, *69*, 297–306, doi:10.1128/IAI.69.1.297.
32. Shen, X., Lagergård, T., Yang, Y., Lindblad, M., Fredriksson, M., Holmgren, J.A.N. Systemic and Mucosal Immune Responses in Mice after Mucosal Immunization with Group B Streptococcus Type III Capsular Polysaccharide-Cholera Toxin B Subunit Conjugate Vaccine. *Infect. Immun.* **2000**, *68*, 5749–5755.

33. Ashoori, Y., Mohkam, M., Heidari, R., Abootalebi, S.N., Mousavi, S.M., Hashemi, S.A., Golkar, N., Gholami, A. Development and In Vivo Characterization of Probiotic Lysate- Treated Chitosan Nanogel as a Novel Biocompatible Formulation for Wound Healing. *Biomed Res. Int.* **2020**, *2020*, 1–9.
34. Gratieri, T., Martins, G., Melani, E., Hugo, V., Freitas, O. De, Fonseca, R., Lopez, V. A Poloxamer / Chitosan in Situ Forming Gel with Prolonged Retention Time for Ocular Delivery. *Eur. J. Pharm. Biopharm.* **2010**, *75*, 186–193, doi:10.1016/j.ejpb.2010.02.011.
35. Khames, A. Investigation of the Effect of Solubility Increase at the Main Absorption Site on Bioavailability of BCS Class II Drug (Risperidone) Using Liquisolid Technique. *Drug Deliv.* **2017**, *24*, 328–338, doi:10.1080/10717544.2016.1250140.
36. Gattefossé *Transcutol ® P For Efficient Drug Solubilization and Skin Penetration*, 2020,
37. Salimi, M., Fouladi, A. Effect of the Various Penetration Enhancers on the in Vitro Skin Permeation of Meloxicam through Whole Rat Skin. *Eur. J. Bio. Pharm. Sci* **2015**, *2*, 1282–1291.
38. Sullivan, D.W., Gad, S.C., Julien, M. A Review of the Nonclinical Safety of Transcutol Ò , a Highly Purified Form of Diethylene Glycol Monoethyl Ether (DEGEE) Used as a Pharmaceutical Excipient. *Food Chem. Toxicol.* **2014**, *72*, 40–50, doi:10.1016/j.fct.2014.06.028.
39. Zirak, M.B., Pezeshki, A. Effect of Surfactant Concentration on the Particle Size, Stability and Potential Zeta of Beta Carotene Nano Lipid Carrier. *Int. J. Curr. Microbiol. Appl. Sci.* **2015**, *4*, 924–932.
40. Softisan Available online: www.warnergraham.com/images/SoftisanHardFatsProdIn.pdf. (accessed on 10 February 2013).
41. Https://Pubchem.Ncbi.Nlm.Nih.Gov/Compound/Glyceryl-Behenate.
42. Gycerol Dibehenate. *Eur. Pharmacop.* 2007.
43. Cirri, M., Mennini, N., Maestrelli, F., Mura, P., Ghelardini, C., Di Cesare Mannelli, L. Development and in Vivo Evaluation of an Innovative “Hydrochlorothiazide-in Cyclodextrins-in Solid Lipid Nanoparticles” Formulation with Sustained Release and Enhanced Oral Bioavailability for Potential Hypertension Treatment in Pediatrics. *Int. J. Pharm.* **2017**, *521*, 73–83.
44. Radomska-Soukharev, A., Muller, R.H. Chemical Stability of Lipid Excipients in SLN-Production of Test Formulations, Characterization and Short-Term Stability. *Pharmazie* **2006**, 425–430.
45. Tan, S.F., Masoumi, H.R.F., Karjiban, R.A., Stanslas, J., Kirby, B.P., Basri, M., Basri, H. Bin Ultrasonic Emulsification of Parenteral Valproic Acid-Loaded Nanoemulsion with Response Surface Methodology and Evaluation of Its Stability. *Ultrason. Sonochem.* **2016**, *29*, 299–308, doi:10.1016/j.ultsonch.2015.09.015.
46. Tang, S.Y., Shridharan, P., Sivakumar, M. Impact of Process Parameters in the Generation of Novel Aspirin Nanoemulsions - Comparative Studies between Ultrasound Cavitation and Microfluidizer. *Ultrason. Sonochem.* **2013**, *20*, 485–497, doi:10.1016/j.ultsonch.2012.04.005.
47. Aoki, M., Ring, T.A., Haggerty, J.S. Analysis and Modeling of the Ultrasonic Dispersion Technique. *Adv. Ceram. Mater.* **1987**, *2*, 209–212.
48. Özdemir, S., Çelik, B., Üner, M. Properties and Therapeutic Potential of Solid Lipid Nanoparticles and Nanostructured Lipid Carriers as Promising Colloidal Drug Delivery Systems. In *Materials for Biomedical Engineering*, 2019, pp. 451–499 ISBN 9780128169131.
49. Moghimi, S.M., Hunter, A.C. Poloxamers and Poloxamines in Nanoparticle Engineering and Experimental Medicine. *TIBTECH* **2000**, *18*, 2958–2964.
50. Han, F., Li, S., Yin, R., Liu, H., Xu, L. Effect of Surfactants on the Formation and Characterization of a New Type of Collodial Drug Delivery System: Nanostructured Lipid Carriers. *Colloids Surfaces A Physicochem. Eng. Asp.* **2008**, *315*, 210–216, doi:10.1016/j.colsurfa.2007.08.005.
51. Appasaheb, P.S. A Review on Intranasal Drug Delivery System. *J. Adv. Pharm. Edu. Res.* **2013**, *3*, 333–346.
52. Thorat, S. Formulation and Product Development of Nasal Spray: An Overview. *Sch. J. Appl. Med. Sci. (SJAMS* **2016**, *4*, 2976–2985, doi:10.21276/sjams.2016.4.8.48.
53. Bunjes, H., Unruh, T. Characterization of Lipid Nanoparticles by Differential Scanning Calorimetry , X-Ray and Neutron Scattering . *Adv. Drug Deliv. Rev.* **2007**, *59*, 379–402, doi:10.1016/j.addr.2007.04.013.

54. Garcia-Fuentes, M., Alonso, M.J., Torres, D. Design and Characterization of a New Drug Nanocarrier Made from Solid–Liquid Lipid Mixtures. *J. Colloid Interface Sci.* **2005**, 590–598.
55. Hu, F.-Q., Jiang, S.-P., Du, Y.-Z., Yuan, H., Ye, Y.Q., Zeng, S. Preparation and Characterization of Stearic Acid Nanostructured Lipid Carriers by Solvent Diffusion Method in an Aqueous System. *Colloids Surf. B Biointerfaces* **2005**, 167–173.
56. Jia, L.-J., Zhang, D.-R., Li, Z.-Y., Feng, F.-F., Wang, Y.-C., Dai, W.-T., Duan, C.-X., Zhang, Q. Preparation and Characterization of Silybin-Loaded Nanostructured Lipid Carriers. *Drug Deliv.* **2010**, *17*, 11–18, doi:10.3109/10717540903431586.
57. Boyer, R.F. Transitions and Relaxations in Amorphous and Semicrystalline Organic Polymers and Copolymers. *Encycl. Polym. Sci. Technol.* 1977, 745–839.
58. Boutonnet-Fagegaltier, N., Menegotto, J., Lamure, A., Duplaa, H., Caron, A., Lacabanne, C., Bauer, M. Molecular Mobility Study of Amorphous and Crystalline Phases of a Pharmaceutical Product by Thermally Stimulated Current Spectrometry. *J. Pharm. Sci.* **2002**, *91*, 1548–1560.
59. Brandl, F., Kastner, F., Gschwind, R.M., Blunk, T., Teßmar, J., Göpferich, A. Release Kinetics. *J. Control. Release* **2009**, *142*, 221–228, doi:10.1016/j.jconrel.2009.10.030.
60. Marx, D., Williams, G., Birkhoff, M. Intranasal Drug Administration - An Attractive Delivery Route for Some Drugs. In *Drug Discovery and Development*, InTech, 2015, pp. 1–23.
61. Basir, R., Rahiman, S.F., Hasballah, K., Chong, W., Talib, H., Yam, M., Jabbarzare, M., Tie, T., Othman, F., Moklas, M., et al. Plasmodium Berghei ANKA Infection in ICR Mice as a Model of Cerebral Malaria. *Iran. J. Parasitol.* **2012**, *7*, 62–74.

Figures

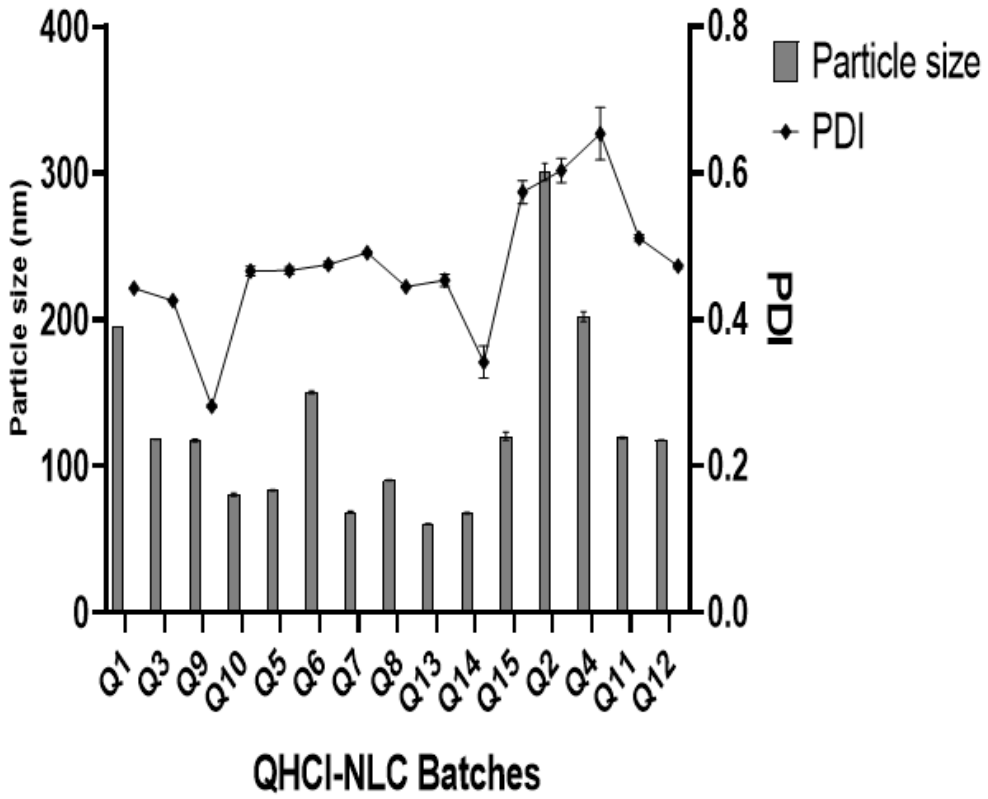

Figure 1

Particle size and PDI of QHCl-NS within 24 h

Key: QHCl = Quinine hydrochloride, S154 = Softisan® 154, C888 = Compritol® 888 ATO, CHD 5 = Compritol® HD 5 ATO. Formulations Q1, Q3, Q9 and Q10 are QHCl-NS made with S154; Q5, Q6, Q7, Q8, Q13, Q14 and Q15 are QHCl-NS made with CHD 5; Q2, Q4, Q11 and Q12 are QHCl-NS made with C888.

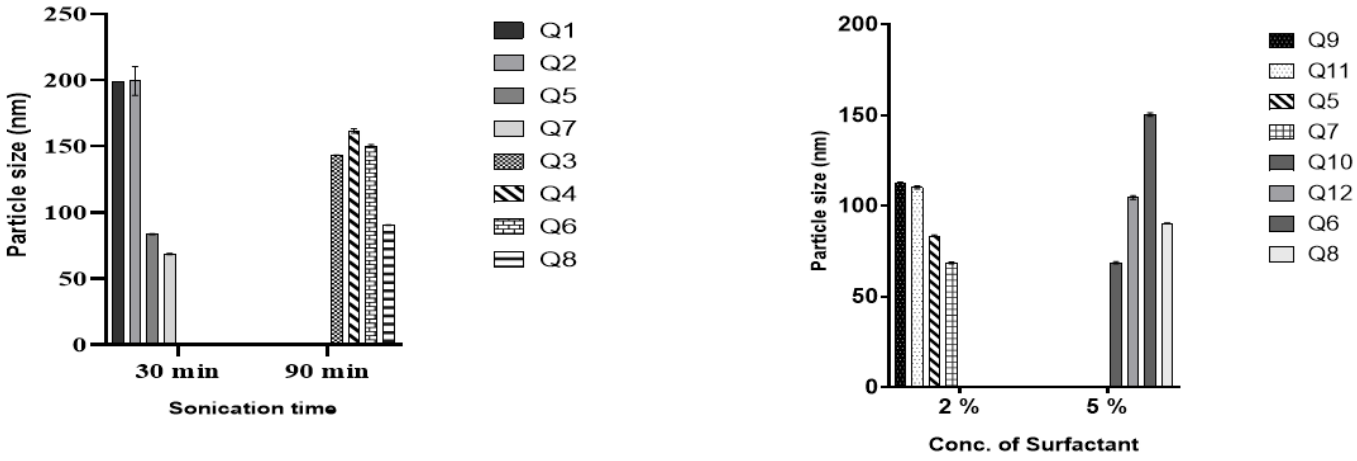

Figure 2

Effect of duration of sonication and concentration of T80 on Particle size of QHCl-NS

Key: QHCl = Quinine hydrochloride, S154 = Softisan® 154, C888 = Compritol® 888 ATO, CHD 5 = Compritol® HD 5 ATO, T80 = Tween® 80. Formulations Q1: contains 1.5 % w/v QHCl, 3 % w/v S154, 2 % w/v T80 and sonicated for 30 min; Q2: contains 1.5 % w/v QHCl, 3 % w/v C888, 2 % w/v T80 and sonicated for 30 min; Q3: contains 1.5 % w/v QHCl, 3 % w/v S154, 2 % w/v T80 and sonicated for 90 min; Q4: contains 1.5 % w/v QHCl, 3 % w/v C888, 2 % w/v T80 and sonicated for 90 min; Q5: contains 1.5 % w/v QHCl, 3 % w/v CHD 5, 2 % w/v T80 and sonicated for 30 min, Q6: contains 1.5 % w/v QHCl, 5 % w/v T80 and sonicated for 30 min; Q7: contains 1.5 % w/v QHCl, 3 % w/v CHD 5, 2 % w/v T80 and sonicated for 90 min; Q8: contains 1.5 %w/v QHCl, 3 % w/v CHD 5, 5 %w/v and sonicated for 90 min. Q5: contains 1.5 % w/v QHCl, 3 % w/v CHD 5, 2 % w/v T80 and sonicated for 30 min, Q6: contains 1.5 % w/v QHCl, 5 % w/v T80 and sonicated for 30 min; Q7: contains 1.5 % w/v QHCl, 3 % w/v CHD 5, 2 % w/v T80 and sonicated for 90 min; NS Q8: contains 1.5 %w/v QHCl, 3 % w/v CHD 5, 5 %w/v and sonicated for 90 min; Q9: contains 1.5 % w/v QHCl, 3 % w/v S154, 2 % w/v T80 and sonicated for 60 min; Q10: contains 1.5 %w/v QHCl, 3 % w/v S154, 5 %w/v and sonicated for 60 min; Q11: contains 1.5 % w/v QHCl, 3 % w/v C888, 2 % w/v T80 and sonicated for 60 min; Q12: contains 1.5 %w/v QHCl, 3 % w/v C888, 5 %w/v and sonicated for 60 min.

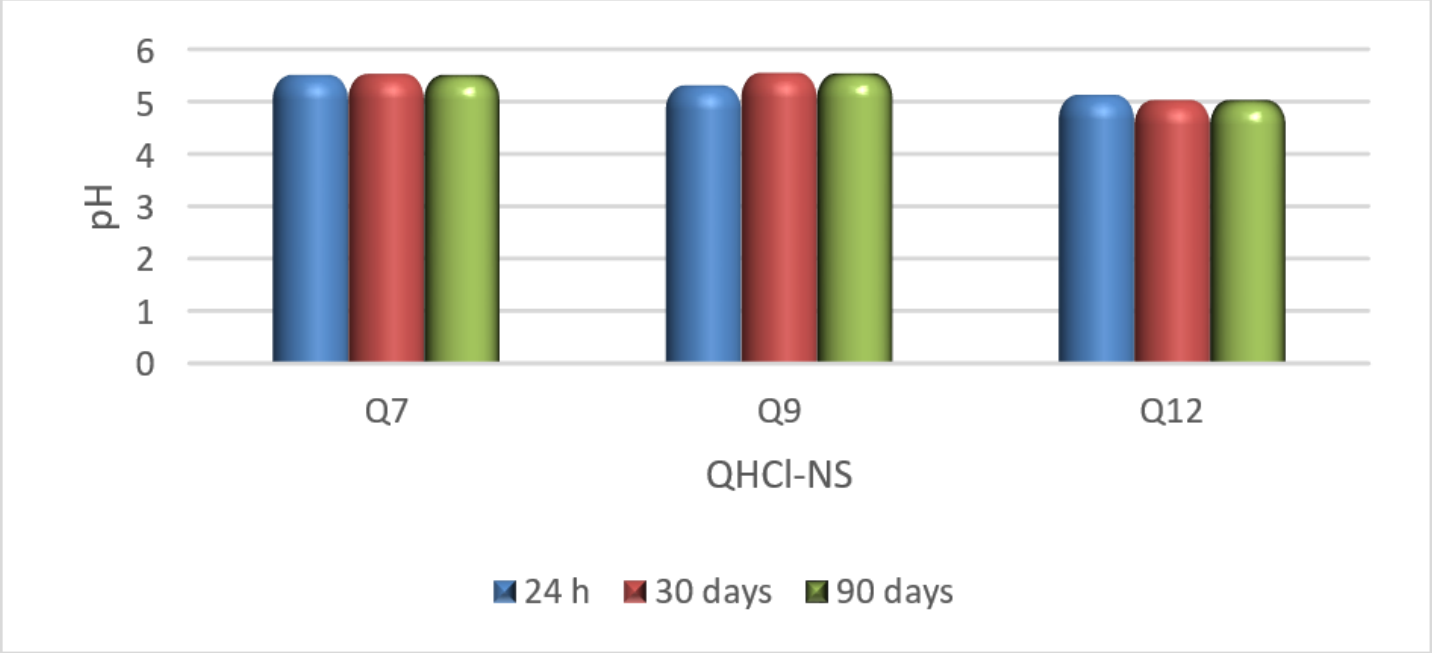

Figure 3

pH stability study of QHCl-NS

Key: QHCl = Quinine hydrochloride, S154 = Softisan® 154, C888 = Compritol® 888 ATO, CHD 5 = Compritol® HD 5 ATO, T80 = Tween® 80. Selected formulations of QHCl-NS = Q7, Q9 and Q12, made with S154, CHD 5 and C888 respectively.

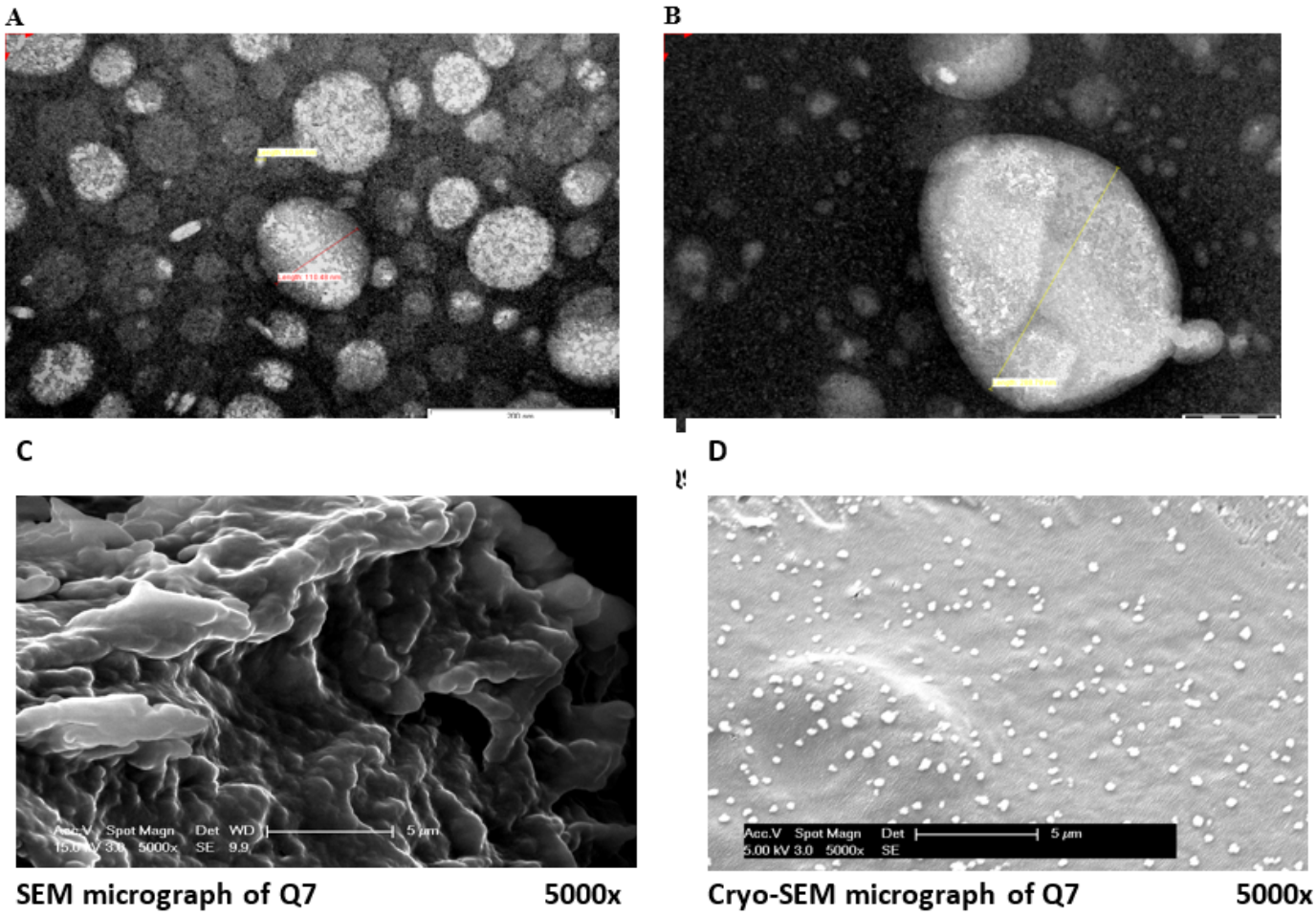

Figure 4

A and B: TEM micrographs of S154 BLANK for QHCl-NS formulations (A) and Q9 (B) (containing 1.5 %w/v QHCl, 3 % w/v S154, 2 % w/v T80 and sonicated for 60 min).

C and D: Comparison between SEM (C) and cryo-SEM (D) micrographs of batch Q7(containing 1.5 % w/v QHCl, 3 % w/v CHD 5, 2 % w/v T80 and sonicated for 90 min)

Key: QHCl = Quinine hydrochloride, S154 = Softisan® 154, C888 = Compritol® 888 ATO, CHD 5 = Compritol® HD 5 ATO, T80 = Tween® 80. Formulations Q9, Q7 and Q12 are QHCl-NS made with S154, CHD 5 and C888, respectively. Plain QHCl, are unprocessed quinine hydrochloride.

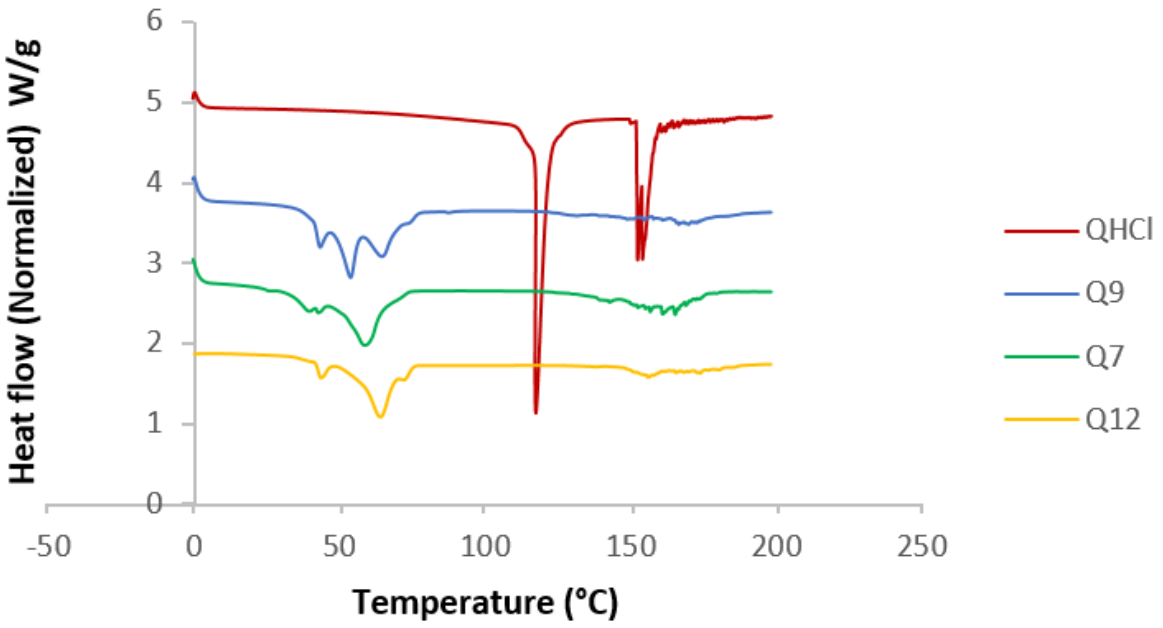

Figure 5

DSC thermogram of selected batches from QHCl-NS

Key: QHCl = Quinine hydrochloride, S154 = Softisan® 154, C888 = Compritol® 888 ATO, CHD 5 = Compritol® HD 5 ATO, T80 = Tween® 80. Formulations Q9, Q7 and Q12 are QHCl-NS made with S154, CHD 5 and C888, respectively.

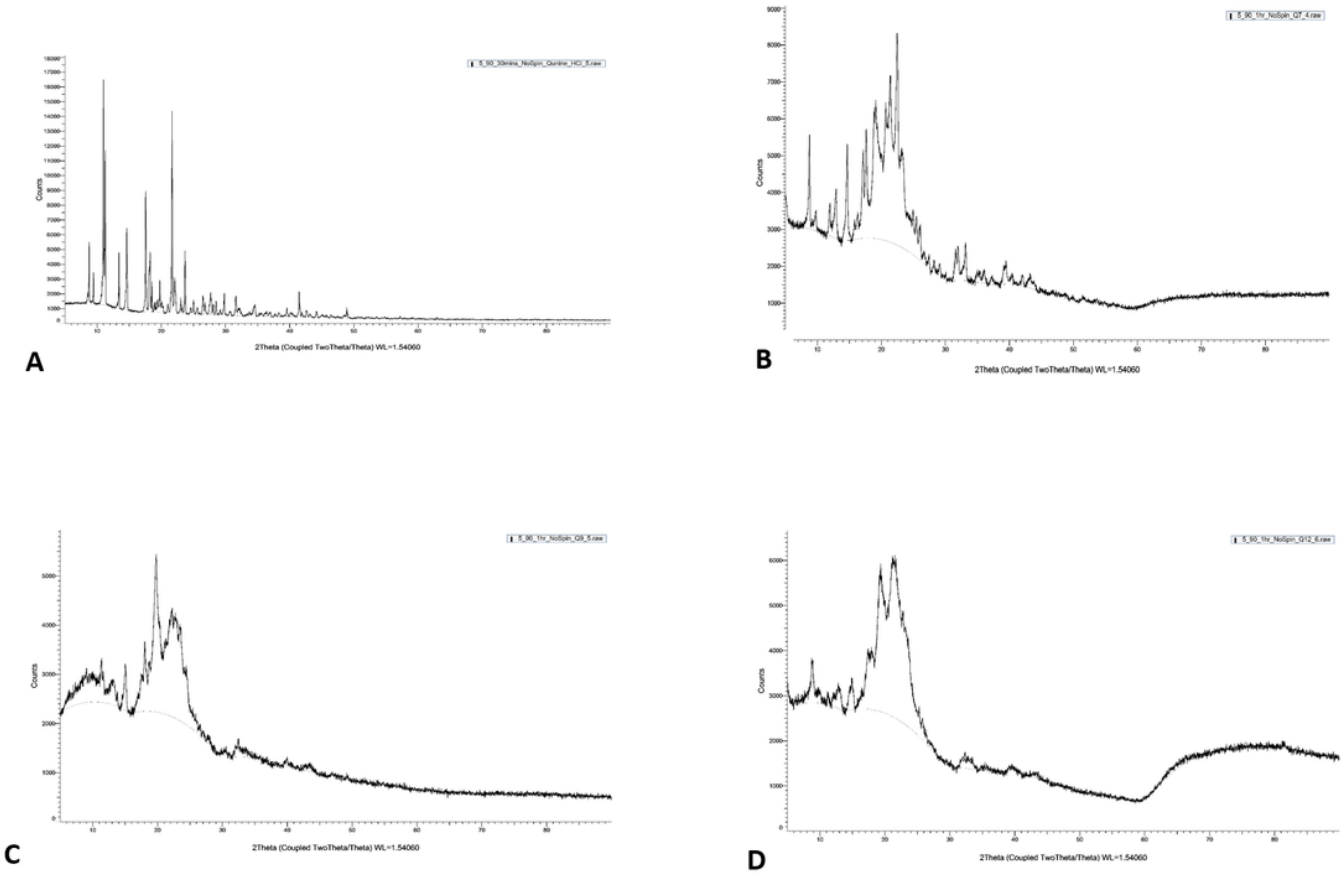

Figure 6

XRD pattern of pure sample of (A) QHCl, (B) Q7, (C) Q9, (D) Q12

Key: QHCl = Quinine hydrochloride, S154 = Softisan® 154, C888 = Compritol® 888 ATO, CHD 5 = Compritol® HD 5 ATO, T80 = Tween® 80. Formulations Q9, Q7 and Q12 are QHCl-NS made with S154, CHD 5 and C888, respectively.

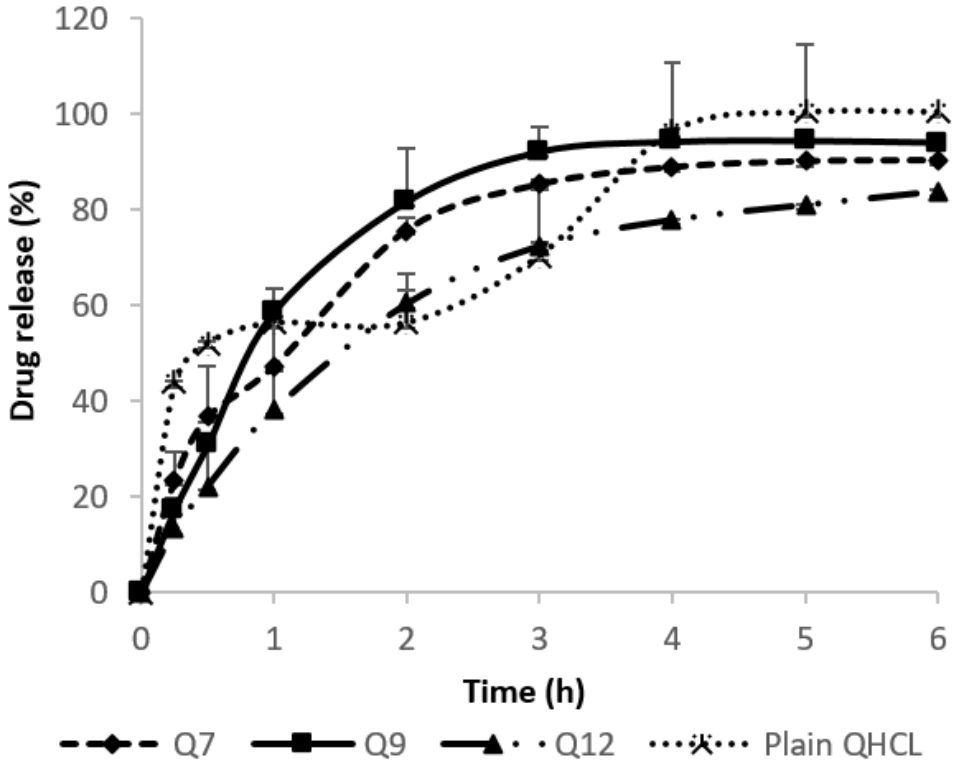

Figure 7

In vitro release of QHCl from NS in simulated nasal fluid

Key: QHCl = Quinine hydrochloride, S154 = Softisan® 154, C888 = Compritol® 888 ATO, CHD 5 = Compritol® HD 5 ATO, T80 = Tween® 80. Formulations Q9, Q7 and Q12 are QHCl-NS made with S154, CHD 5 and C888, respectively. Plain QHCl: unprocessed quinine hydrochloride solution.

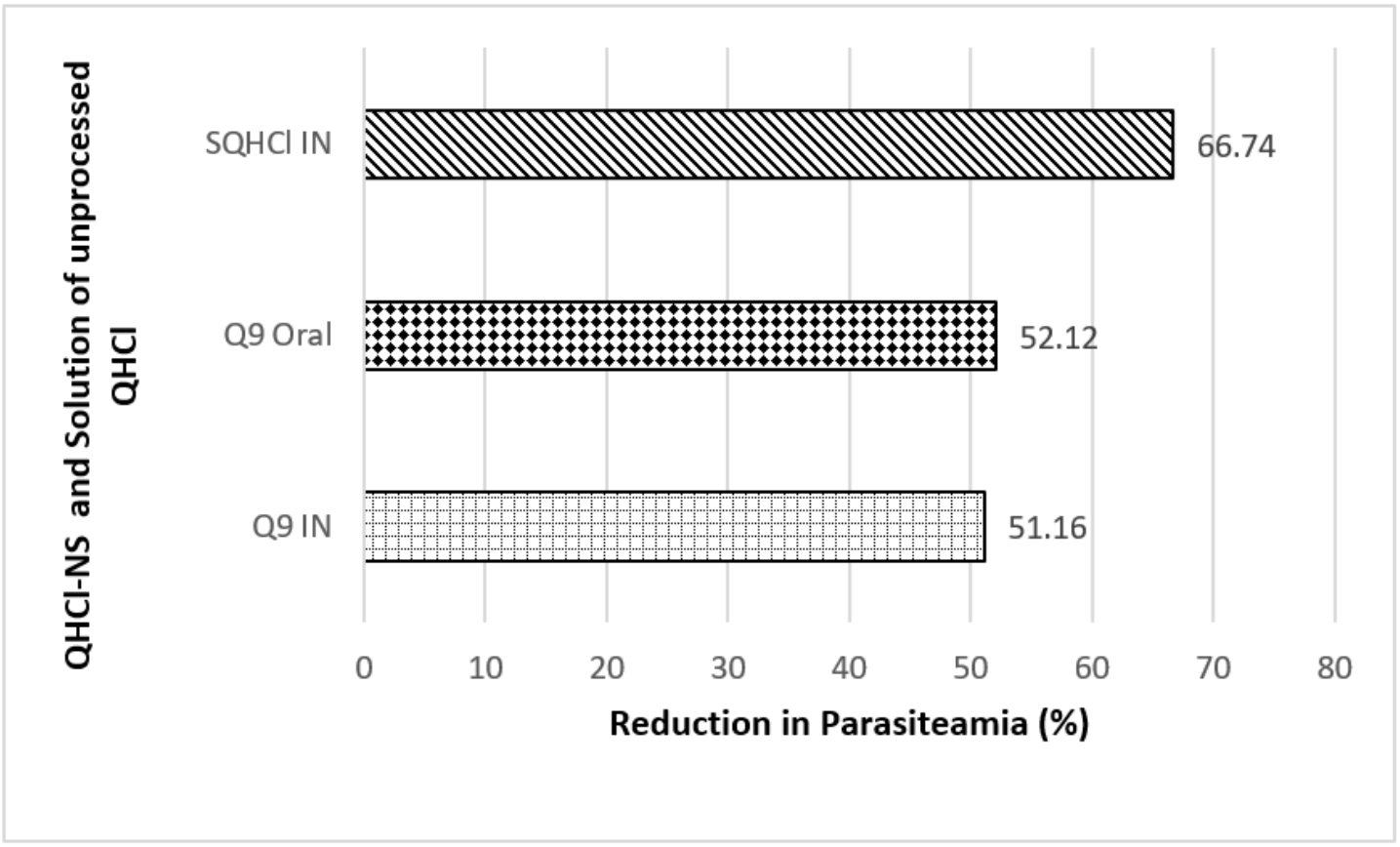

Figure 8

Percentage reduction in parasitaemia after IN and IM treatment with Q9 NS formulation and plain solution of QHCl (SQHCl).

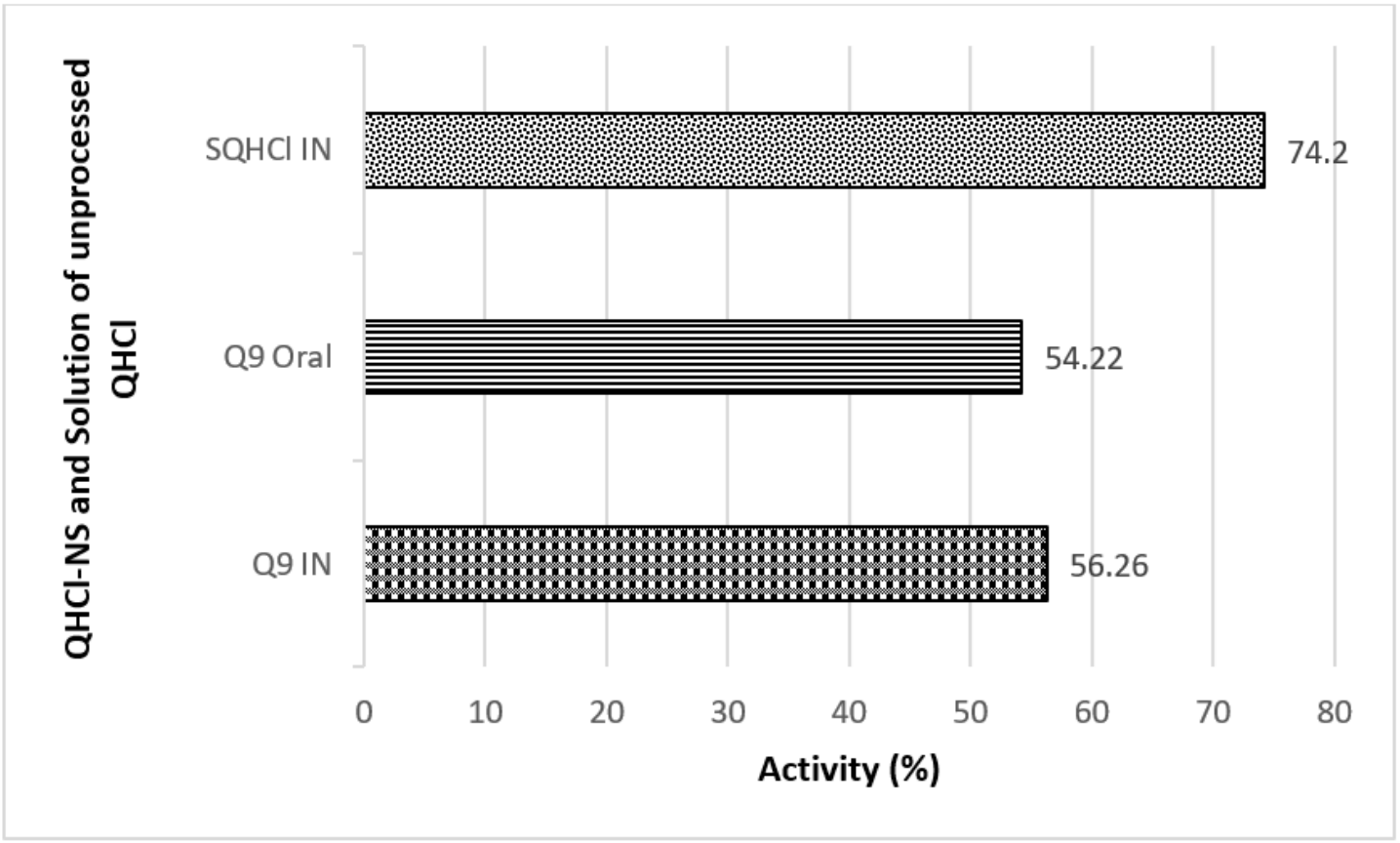

Figure 9

In vivo antimalarial activity after IN and IM treatment with Q9 NS formulation and plain solution of QHCl (SQHCl).

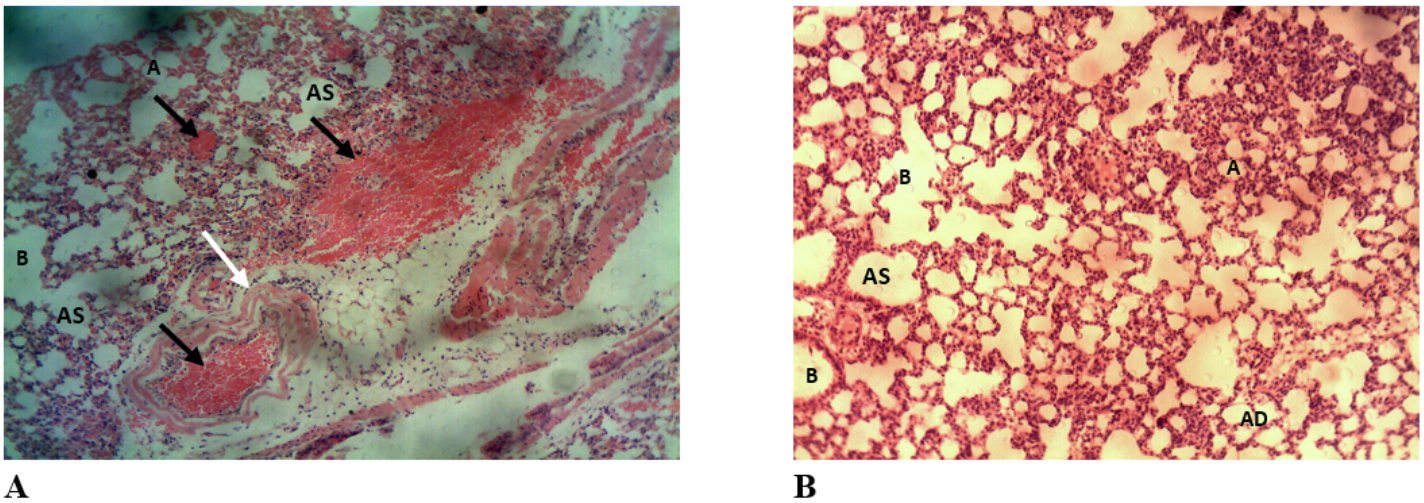

A B

Figure 10

The histomicrograph of the lungs of mice treated with placebo (Fig. 10A) and Q9 (Fig. 10B) showing normal respiratory epithelium of the smaller bronchioles (B) (arrows: ciliated simple columnar epithelium). Note also the normal Alveolar duct (AD), Alveolar sac (AS) and Alveoli (A) in A and B; and the sequestration of parasitized red blood cells (black arrows) and congested

pulmonary vessels (white arrows) in 10A. H & E x100. (For interpretation of the references to colour in this figure legend, the reader is referred to the web version of this article.)

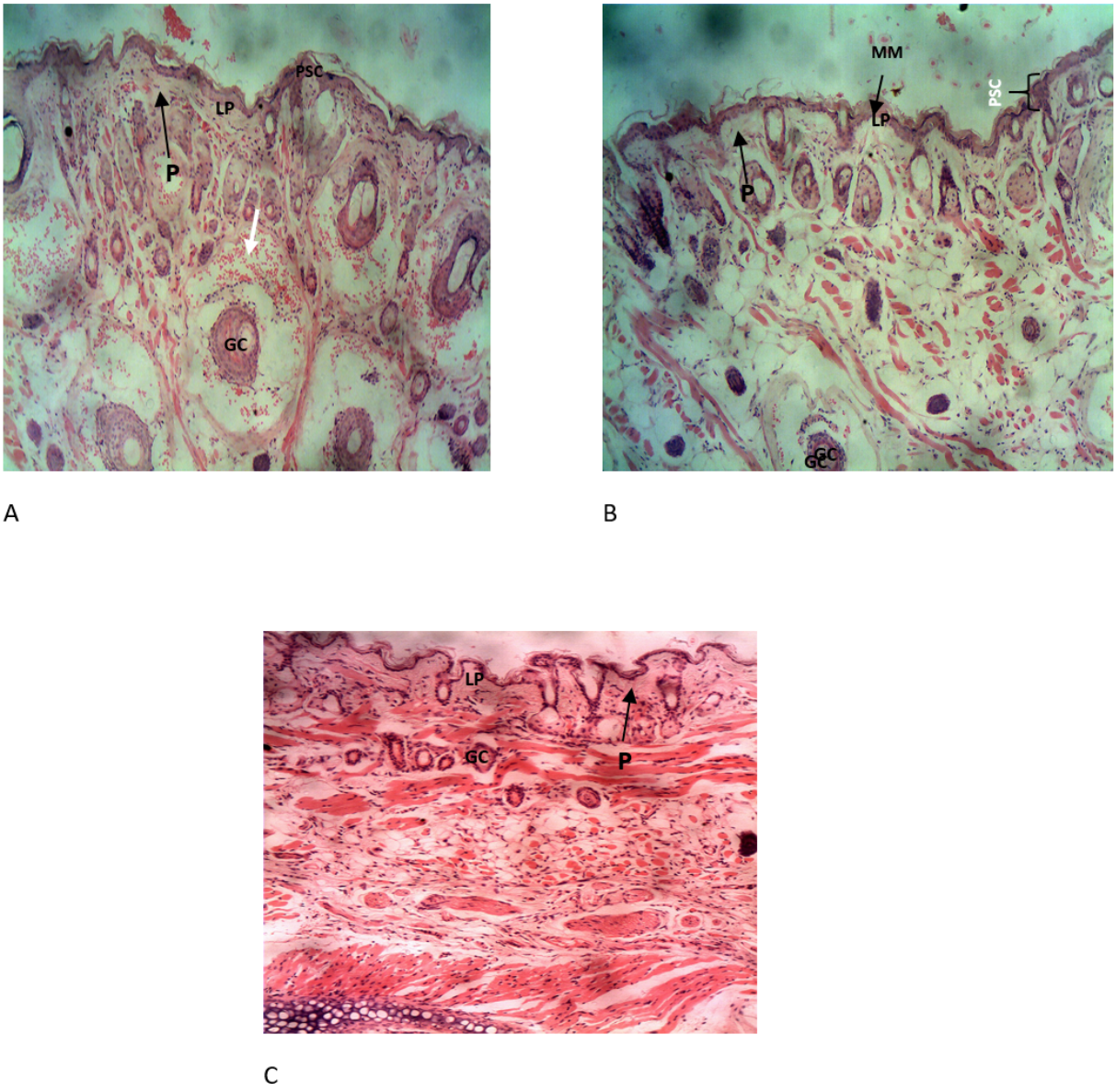

Figure 11

The histomicrograph of the nasal epithelium of mice treated intranasally with placebo (Fig. 11A) and Q9 (Fig. 11B and C) showing the nasal epithelium (epidermis; P) composed of pseudo stratified columnar ciliated epithelium (PSC) and covered by mucus membrane (Fig. 11C; MM). Note also the goblet cells (GC) and the lamina propria (LP). H & E x100 (A and C), x 40 (B). The sequestration of parasitized red blood cells (white arrows).

Supplementary Files

This is a list of supplementary files associated with this preprint. Click to download.

- Appendix.docx